Terrain Relative Navigation for Planetary Landing using Stereo Vision
Measurements Obtained from Hazard Mapping

Woicke, Svenja; Mooij, Erwin

Identification of a Cessna Citation II Model Based on Flight Test Data

M.A. van den Hoek, C.C. de Visser , D.M. Pool

Abstract

As a result of new aviation legislation, from 2019 on all air-carrier pilots are obliged to go through flight simulator-based stall recovery training. For this reason the Control and Simulation division at Delft University of Technology has set up a task force to develop a new methodology for high-fidelity aircraft stall behavior modeling and simulation. As part of this research project, the development of a new high-fidelity Cessna II simulation model, valid throughout the normal, pre-stall flight envelope, is presented in this paper. From an extensive collection of flight test data, aerodynamic model identification was performed using the Two-Step Method. New in this approach is the use of the Unscented Kalman Filter for an improved accuracy and robustness of the state estimation step. Also, for the first time an explicit data-driven model structure selection is presented for the Citation II by making use of an orthogonal regression scheme. This procedure has indicated that most of the six non-dimensional forces and moments can be parametrized sufficiently by a linear model structure. It was shown that only the translational and lateral aerodynamic force models would benefit from the addition of higher order terms, more specifically the squared angle of attack and angle of sideslip. The newly identified aerodynamic model was implemented into an upgraded version of the existing simulation framework and will serve as a basis for the integration of a stall and post-stall model.

M.A. van den Hoek
Delft University of Technology, Delft, The Netherlands e-mail: m.vandenhoek@onderzoeksraad.nl

C.C. de Visser
Delft University of Technology, Delft, The Netherlands e-mail: c.c.devisser@tudelft.nl

D.M. Pool
Delft University of Technology, Delft, The Netherlands e-mail: d.m.pool@tudelft.nl

1 Introduction

A S a result of new aviation legislation, from 2019 on all air-carrier pilots are obliged to go through flight simulator-based stall recovery training [1]. This implies that all aircraft dynamics models driving flight simulators must be updated to include accurate pre-stall, stall, and post-stall dynamics. For this reason, the Control and Simulation (C&S) division at Delft University of Technology has set up a task force to develop a new methodology for high-fidelity aircraft stall behavior modeling and simulation. This research effort is twofold. First, the current simulation framework is to be updated together with the implementation of a newly developed aerodynamic model identified from flight test data obtained from TU Delft's Cessna Citation II laboratory aircraft. As second part of this research effort, an aerodynamic stall model for the Citation II based on flight test data will be developed and integrated into the upgraded simulation framework.

At this moment, the C&S division uses a simulation model of the Cessna Citation I, known as the Delft University Aircraft Simulation Model and Analysis Tool (DASMAT)[2] as its baseline model. This simulation model was designed as standard Flight CAD package for control and design purposes within the C&S division of the Faculty of Aerospace Engineering, Delft University of Technology. DASMAT is known for a number of deficiencies; most significantly is its unsatisfactory match with the current laboratory aircrafts flight dynamics. The Citation I model is the result of a flight test program executed for the development of mathematical models describing the aerodynamic forces and moments, engine performance characteristics, flight control systems and landing gear [3]. Earlier attempts at modeling the longitudinal forces and the pitching moment were made by Oliveira et al.[4]. However, parameter estimates were only obtained for a limited range of flight conditions with a very limited set of measurements. In addition, in the same paper the authors state that dependency of the aerodynamic model from higher order terms, such as α^2 and terms relating to the time rate of change of the aerodynamic angles, such as $\dot{\alpha}$, are yet to be investigated[4].

The estimation of stability and control derivatives from flight test data can be formulated in the framework of maximum likelihood estimation [5]. In the context of this paper, aerodynamic model identification will be done by employing the Two-Step Method (TSM)[6, 7]. This method effectively decomposes the non-linear model identification problem into a non-linear flight path reconstruction problem and linear parameter estimation problem, allowing the use of linear parameter estimation techniques for a significant simplification of the latter procedure. This decomposition can be made under certain conditions concerning accuracy and type of the in-flight measurements[7]. New to the TSM approach is the use of the Unscented Kalman Filter[8] (UKF) for an improved accuracy and robustness of the state estimates in the first step.

2 Research Vehicle and Flight Data

In this paper, aerodynamic model identification was applied to the Cessna Citation II laboratory aircraft, model 550, which is co-owned by Delft University of Technology (DUT) and the Netherlands Aerospace Center (NLR). The Citation II is a twin-jet business aircraft, with two Pratt & Whitney JT15D-4 turbofan engines. Both engines deliver a maximum thrust of 11.1 kN each. The maximum operating speed is limited at 198.6 m/s, with a maximum operating altitude of approximately 13 km [9].

(a) Overview of the aircraft instrumentation systems

(b) Definition of the aircraft body-fixed reference frame or coordinate system $\mathbb{F}_b$
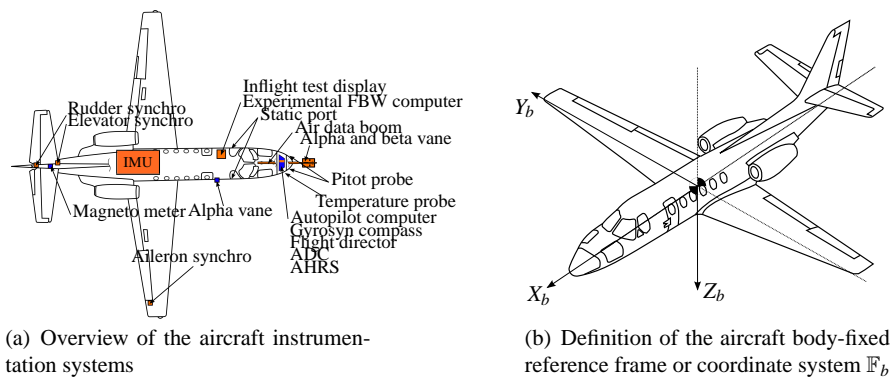
Fig. 1 Aircraft instrumentation systems and reference frame

2.1 Instrumentation

The Flight Test Instrumentation System (FTIS) of the Cessna Citation II laboratory aircraft combines the sensor measurements from a variety of instrumentation systems. An overview of the instrumentation systems is highlighted in Figure 1(a) and summarized in 1.

3 Flight Path Reconstruction

In this section, the methodology for the flight path reconstruction procedure is presented.

Table 1 Flight Test Instrumentation System sensor variables used in flight path reconstruction with their associated 1σ standard deviation and sampling rate F_s.

Parameter	Unit	1σ std	F_s [Hz]	[*]Source
Altitude	m	3.00×10^{-1}	16.67	Static probe
X_b-axis rotation	rad	8.70×10^{-3}	50	Sperry vertical gyro
Y_b-axis rotation	rad	8.70×10^{-3}	50	Sperry vertical gyro
Z_b-axis rotation	rad	1.73×10^{-2}	10	Gyrosyn compass
True airspeed	m/s	1.00×10^{-1}	16.67	Pitot-static probe
Angle of attack	rad	3.50×10^{-3}	1000	Alpha vane
Angle of sideslip	rad	3.50×10^{-3}	1000	Beta vane
X_b-axis linear acceleration	m/s^2	2.00×10^{-2}	100	Q-Flex 3100 accelerometer
Y_b-axis linear acceleration	m/s^2	2.00×10^{-2}	100	Q-Flex 3100 accelerometer
Z_b-axis linear acceleration	m/s^2	3.00×10^{-2}	100	Q-Flex 3100 accelerometer
X_b-axis rotational rate	rad/s	2.00×10^{-3}	100	LITEF μFORS rate gyro
Y_b-axis rotational rate	rad/s	2.00×10^{-3}	100	LITEF μFORS rate gyro
Z_b-axis rotational rate	rad/s	5.00×10^{-3}	100	LITEF μFORS rate gyro

[*] Sampling rate values correspond to the new FTIS. Data obtained from the old FTIS have different sampling rates.

3.1 Kalman Filtering Preliminaries

3.1.1 State transition function and navigation equations

The set of stochastic differential equations, in the context of aircraft dynamics, can in general be described by:

$$
\begin{aligned}
\dot{\mathbf{x}}(t) &= \mathbf{f}\left[\mathbf{x}(t), \mathbf{u}(t), t\right] + \mathbf{G}(\mathbf{x}(t), t)\mathbf{w}(t) \\
\mathbf{z}_n(t) &= \mathbf{h}\left[\mathbf{x}(t), \mathbf{u}(t), t\right] \\
\mathbf{z}(t) &= \mathbf{z}_n(t) + \mathbf{v}(t)
\end{aligned}
\tag{1}
$$

where $\mathbf{f}\left[\cdot\right]$ is the non-linear state transition function and $\mathbf{h}\left[\cdot\right]$ the non-linear measurement function. The process noise and (output) measurement noise are assumed to be zero-mean, white and uncorrelated and can be parametrized by:

$$
\mathbb{E}\left\{\mathbf{v}\mathbf{v}^\mathsf{T}\right\} = \mathbf{Q} \qquad \mathbb{E}\left\{\mathbf{w}\mathbf{w}^\mathsf{T}\right\} = \mathbf{R} \qquad \mathbb{E}\left\{\mathbf{w}\mathbf{v}^\mathsf{T}\right\} = 0
\tag{2}
$$

where the diagonal elements of the process and measurement noise covariance matrices are composed of the squared standard deviation as given in Table 1. The full kinematic model is given by combining the differential equations for the flat earth position, body velocity components and the equations of rotational motion. The whole set of differential equations is then given by:

$$\dot{z}_E = -u\sin\theta + (v\sin\phi + w\cos\phi)\cos\theta \qquad \dot{\phi} = p + q\sin\phi\tan\theta + r\cos\phi\tan\theta$$
$$\dot{u} = a_x - g\sin\theta - qw + rv \qquad \dot{\theta} = q\cos\phi - r\sin\phi \qquad (3)$$
$$\dot{v} = a_y + g\cos\theta\sin\phi - ru + pw \qquad \dot{\psi} = \frac{\sin\phi}{\cos\theta} + r\frac{\cos\phi}{\cos\theta}$$
$$\dot{w} = a_z + g\cos\theta\cos\phi - pv + qu$$

In this set of kinematic equations, the IMU measurements are used as system input. In order to model the noise characteristics and bias of the IMU signals, these were modeled as:

$$a_{x_m} = a_x + \lambda_{a_x} + w_x \qquad\qquad p_m = p + \lambda_p + w_p$$
$$a_{y_m} = a_y + \lambda_{a_y} + w_y \qquad\qquad q_m = q + \lambda_q + w_q \qquad (4)$$
$$a_{z_m} = a_z + \lambda_{a_z} + w_z \qquad\qquad r_m = r + \lambda_r + w_r$$

where λ indicates the bias of the associated signal and w indicates the process noise of the subscripted variable.

In the context of this paper, angle of attack and angle of sideslip measurements were primarily obtained through the use of an intrusive nose boom (see Figure 1(a)). To this end, the set of observation equations was extended by including the equation for the angle of attack and angle of sideslip as measured by the boom [10] including the sensor biases [11]. This model contains an unknown fuselage-upwash coefficient $C_{\alpha_{up}}$ together with a kinematically induced angle of attack and angle of sideslip, under the assumption of a zero vertical wind component and alignment of the boom with the X_b-axis. The complete set of observation equations, or the navigation model, is given by:

$$V_{TAS_m} = \sqrt{u^2 + v^2 + w^2} + v_{V_{TAS}}$$
$$h_m = h + v_h$$
$$\phi_m = \phi + v_\phi \qquad \alpha_v = (1 + C_{\alpha_{up}})\tan^{-1}\frac{w}{u} + \frac{(q - \lambda_q)x_{v_\alpha}}{\sqrt{u^2 + v^2 + w^2}} + v_\alpha$$
$$\theta_m = \theta + v_\theta$$
$$\psi_m = \psi + v_\psi \qquad\qquad (5)$$
$$\beta = \tan^{-1}\frac{v}{\sqrt{u^2 + w^2}} - \frac{(r - \lambda_r)x_{v_\beta}}{\sqrt{u^2 + v^2 + w^2}} + v_\beta$$

where v is the standard notation for the measurement noise of the subscripted variable and x_v denotes the location of the boom along the X_b-axis for the alpha and beta vane.

For use in flight path reconstruction with a Kalman filter, the set of equations in Eq. (3) was extended with the time derivatives of additional states that require reconstruction, i.e. sensor biases. Commonly, the state transition function is simply assumed to be zero since the bias is constant in reality. For increased excitation of the sensor bias state, the state transition function for the linear accelerations and

fuselage-upwash coefficient was modeled as zero-mean unit-variance random walk scaled by a factor k, as earlier applied in the work of Mulder et al.[12]:

$$\dot{\lambda} \sim k \cdot \mathcal{N}(0,1) \tag{6}$$

The bias state transition function for the rotational rates was assumed to be zero for its usually very small bias. On balance, the state vector together with the augmented bias terms is given by:

$$\mathbf{x} = \begin{bmatrix} h \ u \ v \ w \ \phi \ \theta \ \psi \ \lambda_{a_x} \ \lambda_{a_y} \ \lambda_{a_z} \ \lambda_p \ \lambda_q \ \lambda_r \ C_{\alpha_{\mathrm{up}}} \end{bmatrix}^{\mathsf{T}} \tag{7}$$

3.2 Kalman Filtering Procedure

To begin with the formulation of the augmented UKF [8, 13, 14, 15], the augmented state vector and covariance matrix are defined as:

$$\hat{\mathbf{x}}^a(k) = [\hat{\mathbf{x}}(k|k)^{\mathsf{T}} \ \mathbf{v}(k)^{\mathsf{T}} \ \mathbf{w}(k)^{\mathsf{T}}]^{\mathsf{T}} \tag{8}$$

$$\mathbf{P}^a(k) = \begin{bmatrix} \mathbf{P}(k) & 0 & 0 \\ 0 & \mathbf{Q} & 0 \\ 0 & 0 & \mathbf{R} \end{bmatrix} \tag{9}$$

where $\mathbf{v}$ and $\mathbf{w}$ in the augmented state vector represent the means of the process and measurement noise; these can therefore be assumed to have zero mean, hence their values will be zero. The augmented state vector and covariance matrix can then easily be transformed to the unscented domain by:

$$\begin{aligned} \mathscr{X}_i^a(k) &= \left[\hat{\mathbf{x}}^a(k) + \sqrt{(L+\lambda)\mathbf{P}^a(k)} \right] & i = 1,2,\dots,L \\ \mathscr{X}_i^a(k) &= \left[\hat{\mathbf{x}}^a(k) - \sqrt{(L+\lambda)\mathbf{P}^a(k)} \right] & i = L+1,L+2,\dots,2L \end{aligned} \tag{10}$$

This set of transformed points, indicated by $\mathscr{X}^a$, is referred to as the set of sigma points. Parameters L and λ are, respectively, the dimensionality of the state vector and a scaling factor defined as $\lambda = \alpha^2(L+\kappa) - L$. α is a parameter to reflect the spread of the sigma points around its mean, state vector $\hat{\mathbf{x}}$, and β is a factor to account for any prior knowledge. The latter is set to a value of 2 for Gaussian distributions. κ is an extra scaling factor which is usually set to zero. Subsequently, the weights for the set of transformed means and covariances are defined as follows:

$$W_0^{(m)} = \frac{\lambda}{L+\lambda}$$

$$W_0^{(c)} = \frac{\lambda}{L+\lambda} + (1 - \alpha^2 + \beta) \tag{11}$$

$$W_i^{(m)} = W_i^{(c)} = \frac{1}{2(L+\lambda)} \qquad i = 1, 2, \ldots, 2L$$

From this point, the equations of the UKF become more trivial. Analogously to the EKF, the state vector which is now expressed as sigma points are propagated through the system's dynamics:

$$\mathscr{X}^a(k+1|k) = \mathscr{X}^a(k|k) + \int_{t_k}^{t_{k+1}} \mathbf{f}[\mathscr{X}^{a,x}(k|k), \mathbf{u}(k), \mathscr{X}^{a,v}(k|k), \tau]\, d\tau \tag{12}$$

where $\mathscr{X}^{a,x}$ refers to the columns of the sigma points matrix related to the state and superscript v refers to the sigma points related to the process noise. The one step ahead state estimation can be calculated by:

$$\hat{\mathbf{x}}(k+1|k) = \sum_{i=0}^{2L} W_i^{(m)} \mathscr{X}^a(k+1|k) \tag{13}$$

and the one step ahead covariance matrix by:

$$\mathbf{P}(k+1|k) = \sum_{i=0}^{2L} W_i^{(c)} \left(\mathscr{X}_i^{a,x} - \hat{\mathbf{x}}(k|k) \right) \left(\mathscr{X}_i^{a,x} - \hat{\mathbf{x}}(k|k) \right)^{\mathsf{T}} \tag{14}$$

Again, similarly to the EKF, the sigma points representing the state vector and measurement noise are propagated through the measurement equations and subsequently the transformed means for the measurements are calculated:

$$\mathscr{Y}(k+1|k) = \mathbf{h}[\mathscr{X}^{a,x}(k+1|k), \mathscr{X}^{a,w}(k+1|k)] \tag{15}$$

with the transformed measurements given by taking the mean of the transformed sigma points:

$$\hat{\mathbf{y}} = \sum_{i=0}^{2L} W_i^{(m)} \mathscr{Y}_i(k+1|k) \tag{16}$$

The measurement covariance and measurement-state cross-covariance can be calculated by:

$$\mathbf{P_{yy}} = \sum_{i=0}^{2L} W_i^{(c)} \left(\mathscr{Y}_i(k+1|k) - \hat{\mathbf{y}}(k|k) \right) \left(\mathscr{Y}_i(k+1|k) - \hat{\mathbf{y}}(k|k) \right)^{\mathsf{T}} \tag{17}$$

$$\mathbf{P_{xy}} = \sum_{i=0}^{2L} W_i^{(c)} \left(\mathscr{X}_i^{a,x} - \hat{\mathbf{x}}(k|k) \right) \left(\mathscr{Y}_i - \hat{\mathbf{y}}(k|k) \right)^{\mathsf{T}} \tag{18}$$

Finally, to complete the definition of the augmented UKF, gain matrix $\mathscr{K}$, corrected state estimation $\hat{\mathbf{x}}(k+1|k+1)$ and corrected covariance matrix estimation $\mathbf{P}(k+1|k+1)$ are expressed as:

$$\mathscr{K}(k+1) = \mathbf{P_{xy}}\mathbf{P_{yy}^{-1}} \tag{19}$$

$$\hat{\mathbf{x}}(k+1|k+1) = \hat{\mathbf{x}}(k+1|k) + \mathscr{K}\left\{\mathbf{y}(k+1) - \hat{\mathbf{y}}(k+1|k)\right\} \tag{20}$$

$$\mathbf{P}(k+1|k+1) = \mathbf{P}(k+1|k) - \mathscr{K}(k+1)\mathbf{P_{yy}}\mathscr{K}^{\mathsf{T}}(k+1) \tag{21}$$

For additional numerical stability and guaranteed semi-definite state covariance matrix, the square-root implementation of the UKF can be used [16]. This type uses the Cholesky decomposition to address certain numerical advantages in the calculation of the transformed statistical properties. Further extensions to the UKF, e.g. the Sigma-Point Kalman Filter [17] and its iterative counterpart [18] were introduced later. However, these filters populate the whole state-space with sigma points instead of only a selected optimal range. Therefore, the computational burden of such filters do not outweigh the advantages and their application is restricted [19].

4 Aerodynamic Model Identification

4.1 Preliminaries

The six non-dimensional forces and moments can be calculated by:

$$C_X = \frac{m\left(a_x - \lambda_{a_x}\right) - T_x}{\overline{q}S} \tag{22}$$

$$C_Y = \frac{m\left(a_y - \lambda_{a_y}\right)}{\overline{q}S} \tag{23}$$

$$C_Z = \frac{m\left(a_x - \lambda_{a_z}\right)}{\overline{q}S} \tag{24}$$

$$C_l = \frac{I_{xx}}{\overline{q}Sb}\left(\dot{p} - \frac{I_{xz}}{I_{xx}}\left((p - \lambda_p)(q - \lambda_q) + \dot{r}\right) + \frac{I_{zz} - I_{yy}}{I_{xx}}(q - \lambda_q)(r - \lambda_r)\right) \tag{25}$$

$$C_m = \frac{I_{yy}}{\overline{q}Sc}\left(\dot{q} + \frac{I_{xx} - I_{zz}}{I_{yy}}(p - \lambda_p)(r - \lambda_r) + \frac{I_{xz}}{I_{yy}}\left((p - \lambda_p)^2 - (r - \lambda_r)^2\right) - M_T\right) \tag{26}$$

$$C_n = \frac{I_{zz}}{\bar{q}Sb}\left(\dot{r} - \frac{I_{xz}}{I_{zz}}\left(\dot{p} - (q - \lambda_q)(r - \lambda_r)\right) + \frac{I_{yy} - I_{xx}}{I_{zz}}(p - \lambda_p)(q - \lambda_q)\right) \quad (27)$$

where λ denotes the bias obtained from the flight path reconstruction procedure for each of the accelerations and rotational rates. Since the derivatives of the rotational rates are not measured directly, these can be obtained by numerical differentiation. Corrections to the non-dimensional force in X_b and the non-dimensional pitch rate were made by making use of an engine model. The engine-produced thrust in Z_b was neglected and assumed to be approximately zero.

4.2 Parameter Estimation

The principles of regression analysis are well known and previously applied in many different researches in the framework of aerodynamic system identification [20, 21, 22]. The ordinary least squares (OLS) estimator, defined as the minimum residual

$$\Theta_{\text{OLS}} = \min_{\Theta \in \mathbb{R}} \|\mathbf{X} \cdot \Theta - \mathbf{y}\| \quad (28)$$

where $\|\cdot\|$ denotes the L^2 norm in Euclidean space $\mathbb{R}^n$. The well-known solution in terms of linear operations is given by:

$$\hat{\Theta}_{\text{OLS}} = (\mathbf{X}^\mathsf{T}\mathbf{X})^{-1}\mathbf{X}^\mathsf{T}\mathbf{y} \quad (29)$$

According to the Gauss-Markov theorem, the OLS estimator is the best linear unbiased estimator under the assumption that the variance of the residuals should be homoscedastic and the correlation terms should vanish[23]. In addition, under the assumption of a normally distributed residuals vector the OLS estimator is identical to the maximum likelihood estimator, effectively attaining the Cramér-Rao lower bounds (CRLB)[24]. The standard bounds of the parameter estimates are given by the diagonal elements of the variance-covariance matrix:

$$\text{Cov}\{\Theta\} = \mathbb{E}\left\{\left(\hat{\Theta} - \Theta\right)^\mathsf{T}\left(\hat{\Theta} - \Theta\right)\right\} = \sigma^2\left(\mathbf{X}^\mathsf{T}\mathbf{X}\right)^{-1} \quad (30)$$

where σ^2 can be approximated by the mean squared error of the residuals. Using the estimated covariance, pair-wise correlation of the estimated parameters can be assessed by:

$$\text{Corr}\{\hat{\Theta}\} = \begin{pmatrix} \frac{1}{\sigma(\hat{\Theta}_1)} & 0 & \cdots & 0 \\ 0 & \frac{1}{\sigma(\hat{\Theta}_2)} & \cdots & 0 \\ \vdots & \vdots & \ddots & \vdots \\ 0 & 0 & \cdots & \frac{1}{\sigma(\hat{\Theta}_p)} \end{pmatrix} \text{Cov}\{\hat{\Theta}\} \begin{pmatrix} \frac{1}{\sigma(\hat{\Theta}_1)} & 0 & \cdots & 0 \\ 0 & \frac{1}{\sigma(\hat{\Theta}_2)} & \cdots & 0 \\ \vdots & \vdots & \ddots & \vdots \\ 0 & 0 & \cdots & \frac{1}{\sigma(\hat{\Theta}_p)} \end{pmatrix} \quad (31)$$

Because aircraft parameter estimation is often associated with data collinearity[25], a biased parameter estimation technique known as Principal Components Regression (PRC) was used. PCR is able to increase the accuracy of the parameter estimates in case of multi-collinearity among the predictor variables [20].

4.3 Model Structure Selection

Stepwise regression[26] is a method specifically aimed at data-driven selection of an appropriate model structure from a set of candidate regressors. Later modifications to this approach restricted the selection of candidate regressors to higher order terms, starting at a fixed linear model structure[27]. The pool of candidate regressors is to be formed by single terms, cross-interactions and higher order terms corresponding to the independent variables in the model. The downside of the stepwise regression method is that it includes addition and elimination criteria[28]. In addition, regressors cannot be evaluated independently because of their interaction with other regressors in the selected model structure.

More recently, Morelli[21, 29] and Grauer[30] applied a multi-variate polynomial model obtained from an orthogonal model structure selection to various aircraft. The latter model structure selection technique transforms the full set of candidate regressors to the orthogonal domain in order to test the significance of each parameter. By defining a predicted square error (PSE)[30], selection of the orthogonal basis functions can be done by minimization of the latter metric. Terms contributing less than a certain threshold value can also be removed from the model structure.

The process of orthogonal basis functions model structure selection begins with the orthogonalization process of the set of candidate regressors:

$$\mathbf{p}_0 = 1, \quad \mathbf{p}_j = \mathbf{x}_j - \sum_{k=0}^{j-1} \gamma_{kj} \mathbf{p}_k \quad \text{for} \quad j = 1, 2, \dots, n \tag{32}$$

where $\mathbf{x}_j$ is the jth vector of independent variables and coefficient γ_{kj} is defined as:

$$\gamma_{kj} = \frac{\mathbf{p}_k^\mathsf{T} \mathbf{x}_j}{\mathbf{p}_k^\mathsf{T} \mathbf{p}_k} \quad \text{for} \quad k = 0, 1, \dots, j-1 \tag{33}$$

Orthogonal vectors $\mathbf{p}_0, \mathbf{p}_1, \dots, \mathbf{p}_n$ now form the columns of orthogonal regression matrix $\mathbf{P}$. The parameter estimate can now be obtained by the least squares estimator in Eq. (29). This can be done by subsequently calculating the contribution to the total least-squares cost independently for each candidate regressor with:

$$J(\hat{\mathbf{a}}_j) = \frac{\left(\mathbf{p}_j^\mathsf{T} \mathbf{y}\right)^2}{\mathbf{p}_j^\mathsf{T} \mathbf{p}_j} \tag{34}$$

a selection can be made based on the PSE, which is defined as:

$$\text{PSE} = \frac{1}{N}(\mathbf{y} - \hat{\mathbf{y}})^{\mathsf{T}}(\mathbf{y} - \hat{\mathbf{y}}) + \sigma_{\max}^2 \frac{n}{N} \tag{35}$$

The maximum model fit error variance can be obtained from:

$$\sigma_{\max}^2 = \frac{1}{N-1} \sum_{i=1}^{N} (y_i - \bar{\mathbf{y}})^2 \tag{36}$$

5 Results

In this section the results of the flight path reconstruction, model structure selection and parameter estimation procedure are presented. In addition, a comparison between parameter estimates by Koehler and Hardover maneuvers is presented, followed by post identification smoothing of the locally identified models.

5.1 Flight Path Reconstruction

The results for the flight path reconstruction procedure comprises a total of more than 200 individually reconstructed dynamic maneuvers, both longitudinally and laterally induced. For this reason, only a selection of results is shown in this paper. For a typical 3-2-1-1 dynamic maneuver in elevator, the results are depicted in Figure 2. In this figure, the state estimate by the UKF together with the bias estimate, innovation sequences, filtered and reconstructed measurements and the control surface deflections during the maneuver are shown. Innovation sequences are shown to confirm filter consistency.

5.2 Aerodynamic Model Identification

The results from the model structure selection procedure and parameter estimation are presented in this section together with a model validation by applying the identified least squares model to flight derived non-dimensional forces and moments together with a comparison versus the currently implemented aerodynamic model in the DASMAT simulation framework.

The final model structure of the non-dimensional forces and moments in X_b, obtained from an orthogonal least squares model selection scheme, consisted of a total of 5 terms, i.e. C_{X_0}, C_{X_α}, C_{X_q}, $C_{X_{\delta_e}}$, $C_{X_{\alpha^2}}$. However, the term related to the squared angle of attack was removed from the model for its high pairwise correlation with the angle of attack term. Identified values for the parameters as tabulated in Table 2. Tabulated values represent the parameters in the total number of locally identified models. The minimum, maximum and mean values for the estimated parameters
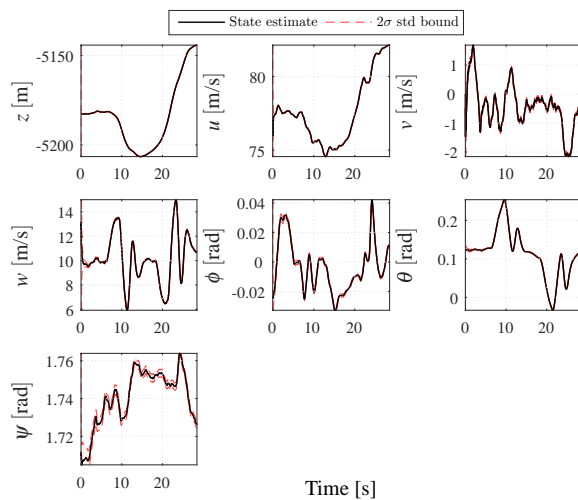
(a) UKF state estimate sequences
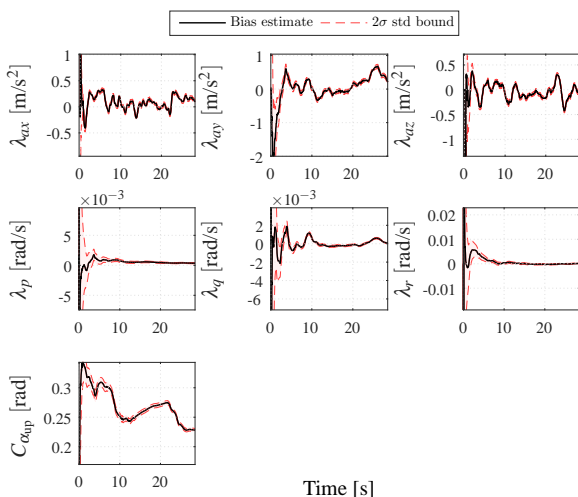
(b) UKF bias estimate sequences
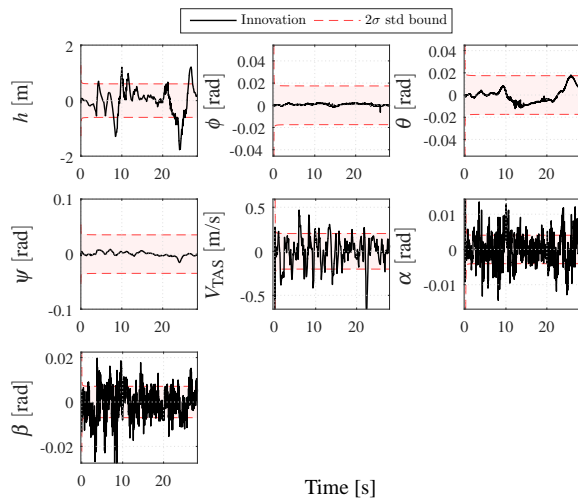
(d) UKF filter innovation sequences

(a) Terms in C_X models

(b) Terms in C_Y models

(c) Terms in C_Z models

(d) Terms in C_l models

(e) Terms in C_m models

(f) Terms in C_n models

Fig. 3 Absolute number of model terms selected in the longitudinal and lateral models obtained from an orthogonal least squares model structure selection procedure.
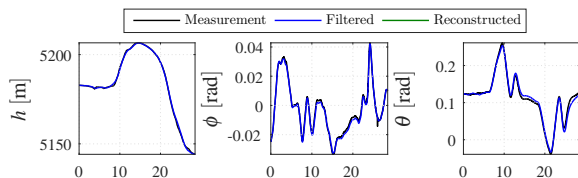
and corresponding variance were included as performance measure to indicate consistence of the estimates.

The models for the 6 dimensionless forces and moments resulting from the model structure selection procedure and parameter estimation were parametrized as follows:

$$C_X = C_{X_0} + C_{X_\alpha} \alpha + C_{X_{\alpha^2}} \alpha^2 + C_{X_q} \hat{q} + C_{X_{\delta_e}} \delta_e \tag{37}$$

$$C_Y = C_{Y_0} + C_{Y_\beta} \beta + C_{Y_p} \hat{p} + C_{Y_r} \hat{r} + C_{Y_{\delta_a}} \delta_a + C_{Y_{\delta_r}} \delta_r + C_{Y_{\beta 2}} \beta^2 \tag{38}$$

$$C_Z = C_{Z_0} + C_{Z_\alpha} \alpha + C_{Z_q} \hat{q} + C_{Z_{\delta_e}} \delta_e \tag{39}$$

$$C_l = C_{l_0} + C_{l_\beta} \beta + C_{l_p} \hat{p} + C_{l_r} \hat{r} + C_{l_{\delta_a}} \delta_a + C_{l_{\delta_r}} \delta_r \tag{40}$$

$$C_m = C_{m_0} + C_{m_\alpha} \alpha + C_{m_q} \hat{q} + C_{m_{\delta_e}} \delta_e \tag{41}$$

$$C_n = C_{n_0} + C_{n_\beta} \beta + C_{n_p} \hat{p} + C_{n_r} \hat{r} + C_{n_{\delta_a}} \delta_a + C_{n_{\delta_r}} \delta_r \tag{42}$$

Table 2 Estimated parameters mean variance, minimum variance and maximum variance for the C_X model, obtained from an orthogonal least squares model structure selection approach.

	$\overline{\theta}$	θ_{min}	θ_{max}	$\overline{\sigma}(\theta)$	$\sigma(\theta)_{min}$	$\sigma(\theta)_{max}$
C_{X_0}	−0.051	−0.594	0.019	1.553×10^{-5}	4.134×10^{-8}	4.710×10^{-4}
C_{X_α}	0.862	−0.213	12.733	1.115×10^{-3}	2.059×10^{-5}	5.349×10^{-2}
C_{X_q}	−4.465	−100.213	17.117	8.591×10^{-1}	1.296×10^{-2}	8.320
$C_{X_{\delta_e}}$	−0.172	−3.602	0.842	2.572×10^{-3}	3.688×10^{-5}	2.736×10^{-2}

Table 3 Estimated parameters mean variance, minimum variance and maximum variance for the C_Y model, obtained from an orthogonal least squares model structure selection approach.

	$\overline{\theta}$	θ_{min}	θ_{max}	$\overline{\sigma}(\theta)$	$\sigma(\theta)_{min}$	$\sigma(\theta)_{max}$
C_{Y_0}	0.004	−0.056	0.059	8.638×10^{-8}	3.190×10^{-10}	8.079×10^{-7}
C_{Y_β}	−0.794	−2.258	−0.169	4.389×10^{-4}	1.362×10^{-6}	4.080×10^{-3}
C_{Y_p}	−0.159	−4.163	2.583	1.403×10^{-2}	3.772×10^{-5}	1.152×10^{-1}
C_{Y_r}	1.958	−1.813	13.569	2.199×10^{-2}	3.163×10^{-5}	1.496×10^{-1}
$C_{Y_{\delta_a}}$	−0.180	−4.305	1.397	2.083×10^{-3}	1.548×10^{-6}	2.282×10^{-2}
$C_{Y_{\delta_r}}$	0.839	−1.988	26.784	4.846×10^{-2}	1.152×10^{-6}	1.427
$C_{Y_{\beta 2}}$	2.754	−14.888	48.476	1.028	2.795×10^{-5}	9.398

Table 4 Estimated parameters mean variance, minimum variance and maximum variance for the C_Z model, obtained from an orthogonal least squares model structure selection approach.

	$\overline{\theta}$	θ_{min}	θ_{max}	$\overline{\sigma}(\theta)$	$\sigma(\theta)_{min}$	$\sigma(\theta)_{max}$
C_{Z_0}	−0.213	−0.941	0.025	1.575×10^{-4}	1.075×10^{-6}	5.183×10^{-3}
C_{Z_α}	−4.037	−8.231	2.868	8.074×10^{-3}	2.369×10^{-4}	4.290×10^{-1}
C_{Z_q}	−57.766	−267.955	189.902	1.320×10^{1}	2.363×10^{-1}	1.979×10^{2}
$C_{Z_{\delta_e}}$	−0.836	−6.355	25.163	4.456×10^{-2}	7.952×10^{-4}	6.847×10^{-1}

Table 5 Estimated parameters mean variance, minimum variance and maximum variance for the C_l model, obtained from an orthogonal least squares model structure selection approach.

	$\overline{\theta}$	θ_{min}	θ_{max}	$\overline{\sigma}(\theta)$	$\sigma(\theta)_{min}$	$\sigma(\theta)_{max}$
C_{l_0}	−0.002	−0.020	0.010	1.826×10^{-8}	1.182×10^{-10}	3.285×10^{-7}
C_{l_β}	−0.073	−0.143	−0.006	1.407×10^{-6}	9.575×10^{-8}	1.490×10^{-5}
C_{l_p}	−0.494	−0.710	0.056	2.656×10^{-5}	1.727×10^{-6}	1.508×10^{-4}
C_{l_r}	0.376	0.024	0.785	6.498×10^{-5}	4.639×10^{-7}	4.298×10^{-4}
$C_{l_{\delta_a}}$	−0.178	−0.276	0.121	6.081×10^{-6}	1.585×10^{-7}	9.996×10^{-5}
$C_{l_{\delta_r}}$	0.102	−1.309	2.314	6.865×10^{-4}	2.784×10^{-8}	1.619×10^{-2}

Table 6 Estimated parameters mean variance, minimum variance and maximum variance for the C_m model, obtained from an orthogonal least squares model structure selection approach.

	$\overline{\theta}$	θ_{min}	θ_{max}	$\overline{\sigma}(\theta)$	$\sigma(\theta)_{min}$	$\sigma(\theta)_{max}$
C_{m_0}	0.021	−0.022	0.089	4.918×10^{-7}	1.252×10^{-8}	5.698×10^{-6}
C_{m_α}	−0.488	−0.855	−0.253	2.509×10^{-5}	2.856×10^{-6}	1.904×10^{-4}
C_{m_q}	−11.935	−22.066	−1.489	3.466×10^{-2}	2.968×10^{-3}	2.920×10^{-1}
$C_{m_{\delta_e}}$	−1.250	−1.508	−0.351	1.204×10^{-4}	9.907×10^{-6}	1.097×10^{-3}

Table 7 Estimated parameters mean variance, minimum variance and maximum variance for the C_n model, obtained from an orthogonal least squares model structure selection approach.

	$\overline{\theta}$	θ_{min}	θ_{max}	$\overline{\sigma}(\theta)$	$\sigma(\theta)_{min}$	$\sigma(\theta)_{max}$
C_{n_0}	0.000	−0.002	0.002	1.158×10^{-8}	2.084×10^{-10}	1.326×10^{-7}
C_{n_β}	0.079	−0.056	0.145	3.689×10^{-6}	1.548×10^{-7}	5.965×10^{-5}
C_{n_p}	−0.142	−0.677	0.284	1.307×10^{-4}	5.361×10^{-6}	3.267×10^{-3}
C_{n_r}	−0.295	−0.474	0.374	1.005×10^{-4}	3.055×10^{-6}	5.440×10^{-4}
$C_{n_{\delta_a}}$	−0.025	−0.155	0.073	4.720×10^{-5}	5.616×10^{-7}	1.049×10^{-3}
$C_{n_{\delta_r}}$	−0.065	−0.611	0.578	7.338×10^{-4}	1.783×10^{-7}	1.770×10^{-2}

5.3 Model Validation

The identified models for all six non-dimensional forces and moments were applied to an independent validation data set consisting of 20% of the total data set. A comparison between the aircraft derived forces and moments, the least squares model and the DASMAT model which is currently implemented in the simulation framework is shown in Figure 4. In addition, fit statistics in terms of the coefficient of determination and the relative root mean square error (RRMSE) are tabulated in Table 8.

A time-domain comparison between the new least-squares model and DASMAT for a longitudinally induced 3-2-1-1 maneuver is presented in Figure 5. This figure indicates an increased fidelity of the predicted aircraft states by the new least-squares model in comparison to the DASMAT model. Most significant is the better fit of the new model for the velocity in the direction of the X_b axis and the Euler angles.

Table 8 Fit statistics for the least squares model and the existing DASMAT (D) model averaged over all validation sets.

	C_X	C_Y	C_Z	C_l	C_m	C_n
R^2	0.76	0.77	0.77	0.75	0.76	0.85
R_D^2	0.60	0.55	0.64	0.25	0.00	0.50
$RRMSE$ (%)	6.76	5.32	6.38	4.96	5.8	4.72
$RRMSE_D$ (%)	8.79	7.34	7.97	8.65	12.65	8.50

6 Conclusion

In this paper, the methodology regarding the identification of an aerodynamic model for flight simulation training from flight test data was developed for the normal post-stall flight envelope. By employing the Two-Step Method (TSM), the Unscented Kalman Filter (UKF) was used in cooperation with linear parameter estimation techniques. Results indicate that the state estimates and measurement reconstructions by the UKF are in good agreement with the presented data.

This research effort results in a simple and parsimonious set of aerodynamic models describing the 6 non-dimensional forces and moments. The model presented in this paper outperforms the current aerodynamic model implemented in the DAS-MAT framework in terms of goodness of fit, in all 6 degrees of freedom, when compared to the recorded forces and moments of the Cessna Citation II laboratory aircraft. The explained variance of the non-dimensional forces was increased with at least 13%. More significant improvements were made to the non-dimensional moments; an increase of the explained variance of at least 35% was achieved.
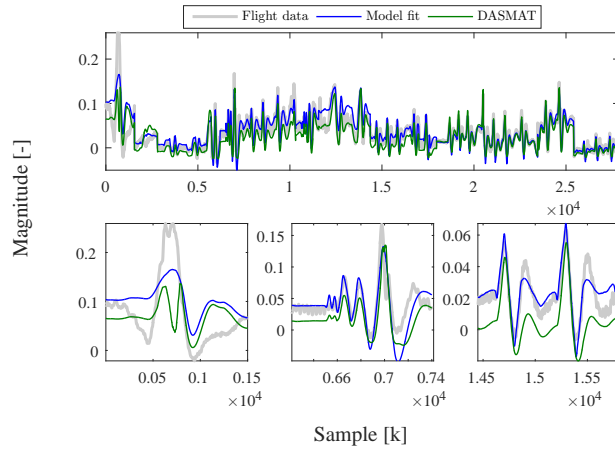
(a) Identified C_X model applied to a validation set
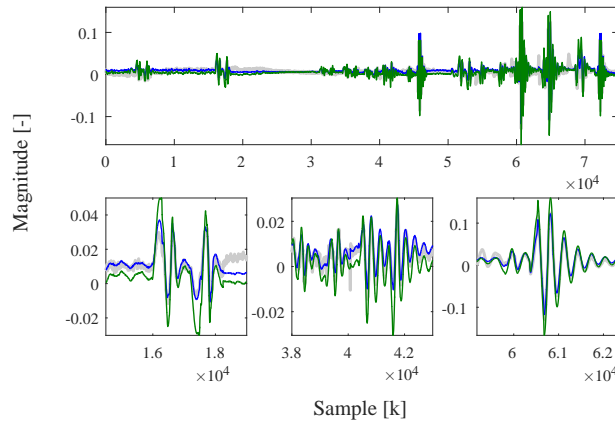
(b) Identified C_Y model applied to a validation set
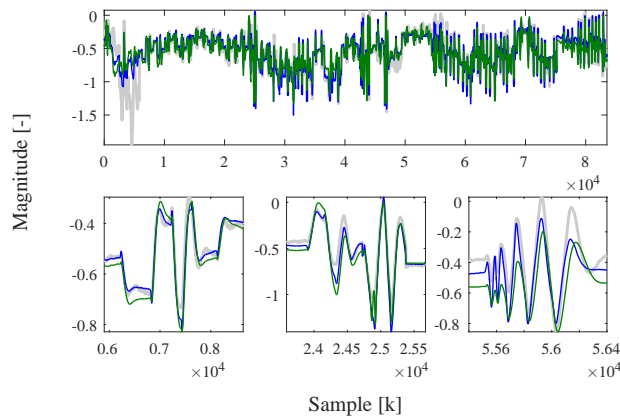
(c) Identified C_Z model applied to a validation set
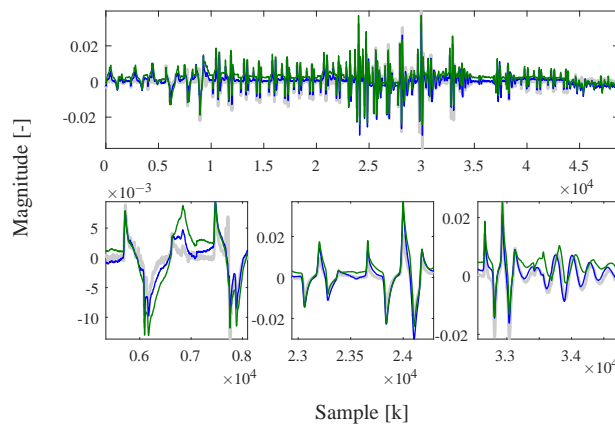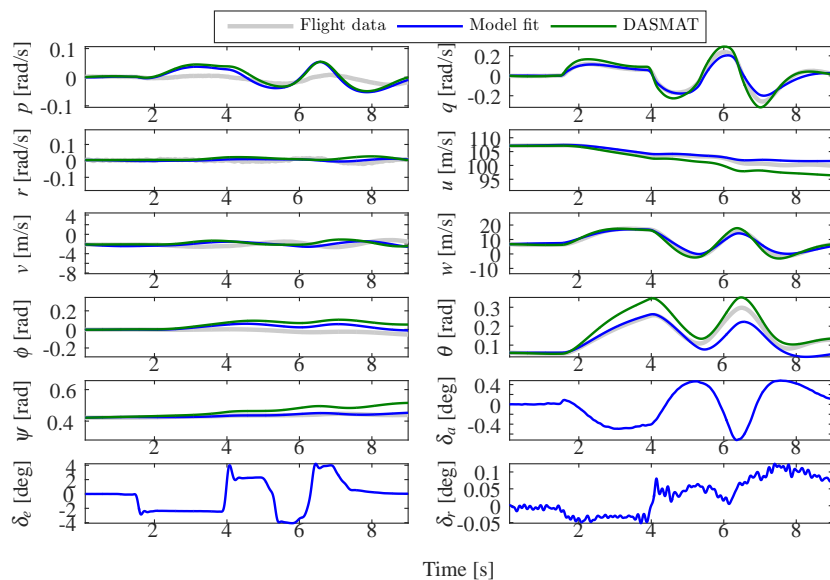
Fig. 5 Time domain response of the newly implemented aerodynamic model together with the currently implemented aerodynamic model in the DASMAT simulation framework and the flight derived aircraft states and control surface deflections for a longitudinally induced δ_e 3-2-1-1 maneuver.

The work presented in this paper will serve as a basis for the integration of a stall and post-stall model, resulting from a parallel research effort. Together, these models will be used in future research into, e.g., the behavior of pilots during aerodynamic stall and the development of new control algorithms.

References

1. Federal Aviation Administration, "Qualification, Service, and Use of Crewmembers and Aircraft Dispatchers," Tech. rep., U.S. Department of Transportation, 2013.
2. van der Linden, C. A. A. M., *DASMAT - Delft University Aircraft Simulation Model and Analysis Tool*, Delft University Press, Delft, 1998.
3. Mulder, J. A., Baarspul, M., Breeman, J. H., Nieuwpoort, A. M. H., Verbaak, J. P. F., and Steeman, P. S. J. M., "Determination of the mathematical model for the new Dutch government civil aviation flying school flight simulator," *Society of Flight Test Engineers, 18th Annual symposium*, Delft University of Technology, Amsterdam, 1987.
4. Oliveira, J., Chu, Q. P., Mulder, J. A., Balini, H. M. N. K., and Vos, W. G. M., "Output error method and two step method for aerodynamic model identification," *AIAA Guidance, Navigation, and Control Conference and Exhibit*, , No. August, 2005, pp. 1–9.
5. Nahi, N. E., *Estimation theory and applications*, John Wiley & Sons, New York, 1969.
6. Mulder, J. A., Chu, Q. P., Sridhar, J. K., Breeman, J. H., and Laban, M., "Non-linear aircraft flight path reconstruction review and new advances," *Progress in Aerospace Sciences*, Vol. 35, No. 7, 1999, pp. 673–726.
7. Mulder, J. A., Sridhar, J. K., and Breeman, J. H., *Identification of Dynamic Systems- Applications to Aircraft Part 2: Nonlinear Analysis and Manoeuvre Design*, Vol. 3, North Atlantic Treaty Organisation, Neuilly Sur Seine, 1994.
8. Julier, S. J. and Uhlmann, J. K., "A New Extension of the Kalman Filter to Nonlinear Systems," *International Symposium for Aerospace Defense Sensing Simulutation and Controls*, Vol. 3, No. 2, 1997, pp. 26.
9. Cessna Aircraft Company, "Operating Manual Model 550 Citation II, Unit -0627 And On," Tech. rep., Wichita, Kansas, USA, 1990.
10. Laban, M., *On-Line Aircraft Aerodynamic Model Identification*, Ph.d. thesis, Delft University of Technology, Delft, 1994.
11. de Visser, C. C., *Global Nonlinear Model Identification with Multivariate Splines*, Ph.D. thesis, Delft University of Technology, Delft, 2011.
12. Mulder, M., Lubbers, B., Zaal, P. M. T., van Paassen, M. M., and Mulder, J. A., "Aerodynamic Hinge Moment Coefficient Estimation Using Automatic Fly-by-Wire Control Inputs," *Proceedings of the AIAA Modeling and Simulation Technologies Conference and Exhibit, Chicago (IL)*, No. AIAA-2009-5692, 2009.
13. Chowdhary, G. and Jategaonkar, R., "Aerodynamic parameter estimation from flight data applying extended and unscented Kalman filter," *Aerospace Science and Technology*, Vol. 14, No. 2, 2010, pp. 106–117.
14. Julier, S. J. and Uhlmann, J. K., "Unscented filtering and nonlinear estimation," *Proceedings of the IEEE*, Vol. 92, No. 3, 2004, pp. 401–422.
15. Wan, E. A. and Van Der Merwe, R., "The unscented Kalman filter for nonlinear estimation," *Adaptive Systems for Signal Processing, Communications, and Control Symposium 2000. AS-SPCC. The IEEE 2000*, 2002, pp. 153–158.
16. Van Der Merwe, R. and Wan, E. A., "The square-root unscented Kalman filter for state and parameter-estimation," *Acoustics, Speech, and Signal Processing, 2001. Proceedings. (ICASSP '01). 2001 IEEE International Conference on*, Vol. 6, 2001, pp. 3461–3464 vol.6.
17. van der Merwe, R. and Wan, E. A., "Sigma-Point Kalman Filters for Integrated Navigation," *Proceedings of the 60th Annual Meeting of the Institute of Navigation (ION)*, 2004, pp. 641–654.
18. Sibley, G., Sukhatme, G. S., and Matthies, L. H., "The Iterated Sigma Point Kalman Filter with Applications to Long Range Stereo," *Rss*, 2006.
19. Armesto, L., Tornero, J., and Vincze, M., "On multi-rate fusion for non-linear sampled-data systems: Application to a 6D tracking system," *Robotics and Autonomous Systems*, Vol. 56, No. 8, 2008, pp. 706–715.

20. Klein, V., "Estimation of aircraft aerodynamic parameters from flight data," *Progress in Aerospace Sciences*, Vol. 26, No. 1, 1989, pp. 1–77.
21. Morelli, E. A., "Global nonlinear parametric modelling with application to F-16 aerodynamics," *American Control Conference, 1998. Proceedings of the 1998*, Vol. 2, jun 1998, pp. 997–1001 vol.2.
22. Morelli, E. and Derry, S. D., "Aerodynamic Parameter Estimation for the X-43A (Hyper-X) from Flight Data," *AIAA Atmosperic FlightMechanics Conference and Exhibit*, , No. August, 2005.
23. Goldberg, M. A. and Cho, H. A., *Introduction to Regression Analysis*, WIT Press, Southampton, UK, 2003.
24. Watson, P. K. and Teelucksingh, S. S., *A Practical Introduction to Econometric Methods: Classical and Modern*, University of the West Indies Press, 2002.
25. Morelli, E. A., "Practical Aspects of the Equation-Error Method for Aircraft Parameter Estimation," *AIAA Atmospheric Flight Mechanics Conference*, , No. 6114, 2006, pp. 1–18.
26. Batterson, J. G. and Klein, V., "Partitioning of flight data for aerodynamic modeling of aircraft at high angles of attack," *Journal of Aircraft*, Vol. 26, No. 4, apr 1989, pp. 334–339.
27. Klein, V., Batterson, J. G., and Murphy, P. C., "Determination of airplane model structure from flight data by using modified stepwise regression," Tech. rep., NASA Langley Research Center, Hampton, 1981.
28. Lombaerts, T., Oort, E. V., Chu, Q. P., Mulder, J. A., and Joosten, D., "Online Aerodynamic Model Structure Selection and Parameter Estimation for Fault Tolerant Control," *Journal of Guidance, Control, and Dynamics*, Vol. 33, No. 3, 2010, pp. 707–723.
29. Morelli, E., "Efficient Global Aerodynamic Modeling from Flight Data," *50th AIAA Aerospace Sciences Meeting including the New Horizons Forum and Aerospace Exposition*, Aerospace Sciences Meetings, American Institute of Aeronautics and Astronautics, jan 2012.
30. Grauer, J. A. and Morelli, E. A., "Generic Global Aerodynamic Model for Aircraft," *Journal of Aircraft*, Vol. 52, No. 1, jul 2014, pp. 13–20.